

Chapter 4

Interacting Particle Systems

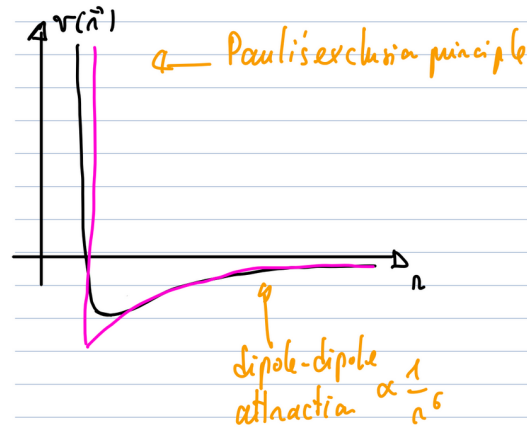


Figure 4.1: Sketch of the Lennard Jones potential.

So far we have studied a beautiful self-consistent theory that works for dilute and relative simple systems. However, the world around us is rich and complex because **more is different**. It is the interplay between fluctuations and interactions that enables matter to take complex forms. In this Chapter, we consider the following questions:

- How do we account for the interactions?
- What new phenomena do they lead to?

We do so in the context of the liquid-gas phase transition in Section 4.1 and of the ferromagnetic transition using the celebrated Ising model in Section 4.2

4.1 Interacting fluids: liquid-gas phase separation

We consider an equilibrium fluid comprising N particles, whose hamiltonian reads:

$$H = \underbrace{\sum_{i=1}^N \frac{\vec{p}_i^2}{2m}}_{\text{kinetic energy}} + \underbrace{\sum_{i < j} v(\vec{q}_i - \vec{q}_j)}_{\text{pairwise potential}}, \quad (4.1)$$

where the pairwise potential takes into account both short range repulsion among the particles due to Pauli exclusion principle, and long-range attractive forces due to dipole-dipole interactions. A common potential to describe such interactions, that are common in atomic fluids, is the **Lennard Jones potential**:

$$v(r) = \frac{\varepsilon}{4} \left[\left(\frac{\sigma}{r} \right)^{12} - \left(\frac{\sigma}{r} \right)^6 \right] \quad (4.2)$$

with r is the distance between the particles (See Fig 4.1).

For such systems, a transition from a gas phase to a liquid phase is observed at low enough temperatures (see Figure 4.2). In the canonical ensemble, as the density increases away from the dilute gas limit, one observes the nucleation of small liquid droplets at a gas density $n_G(T)$, called the "gas binodal". Inside the liquid droplet, the density is $n_L(T)$, which is called the "liquid binodal". As the average density increases

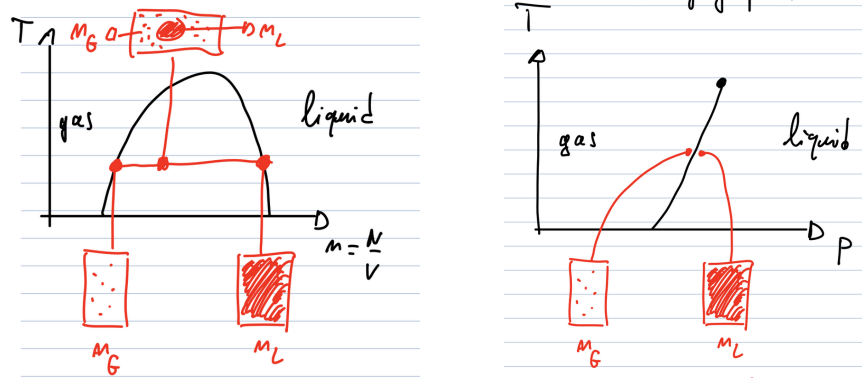


Figure 4.2: **Left:** In the canonical ensemble one controls the temperature T and the density $n = N/V$. In this case, at low temperature, the system undergoes phase separation between a homogeneous gas phase with density $n_G(T)$ and a liquid phase with density $n_L(T) > n_G$. **Right:** In the isobaric ensemble, one controls the temperature T and the pressure P . In this case, the density of the system is allowed to fluctuate and one does not observe phase coexistence. The system instead jumps discontinuously from the gas phase to the liquid phase when increasing the pressure and crossing the transition line.

from n_G to n_L , the system remains phase separated and liquid and gas phases coexist. Each phase keeps its density constant as the average density increases. As a result, the size of the liquid droplets increases. When the system reaches the density $n_L(T)$, the liquid phase fills the entire space and one observes a uniform system again.

Note that the term "liquid" and "gas" are simply used to distinguish the dense and dilute coexisting phases. Apart from the average distance between atoms, no symmetry breaking distinguishes these two fluid phases.

In the isobaric ensemble, when one fixes N , T and P instead of N , T and V , the story is a little bit different. At very low pressure, the system is dilute and homogeneous. As P increases, the density of the system continuously increases until a value $P_t(T, N)$ where the density discontinuously jumps from the value $n_G(T)$ to the value $n_L(T)$. The phase-coexistence scenario of the canonical ensemble has been replaced by a discontinuous phase transition. A similar discontinuous transition would be observed in the grand-canonical ensemble upon increasing μ .

The goal of this section is to build a predictive theory for the transition observed in the isobaric ensemble. The transition in the canonical ensemble is studied in Exercise 1 of Pset 7.

4.1.1 The virial expansion

To make progress, let us try to compute the **canonical partition function**:

$$Z = \frac{1}{N!} \int \prod_{i=1}^N \frac{d^3 \vec{q}_i d^3 \vec{p}_i}{h^3} e^{-\beta \sum_{i=1}^N \frac{p_i^2}{2m}} e^{-\beta \sum_{i < j} v(\vec{q}_i - \vec{q}_j)} = \frac{1}{N! \Lambda^{3N}} \underbrace{\int \prod_{i=1}^N d^3 \vec{q}_i \prod_{i < j} e^{-\beta v(\vec{q}_i - \vec{q}_j)}}_{\text{difficult to compute}} \quad (4.3)$$

with $\Lambda = \sqrt{\frac{h^2}{2\pi m k_B T}}$ the thermal De Broglie wavelength. The limit that we can treat analytically is the **dilute limit** where $e^{-\beta v} \simeq 1$ since particles are very far apart.

To make progress beyond this limit, we can try to develop a **perturbation theory**. We thus write:

$$e^{-\beta v(\vec{q}_i - \vec{q}_j)} = 1 + \left(e^{-\beta v(\vec{q}_i - \vec{q}_j)} - 1 \right) \equiv 1 + f_{ij}, \quad (4.4)$$

where the last equality is the definition for f_{ij} . The underlying idea is that, in the low-but-finite density limit, the f_{ij} will not contribute much, but they will tell us about how interactions modify the ideal gas picture, hopefully suggesting a way to describe the phase transition.

To characterize what happens as density increases, we aim to express the physical observables of our system as a series in the number density n . For the **pressure**, the corresponding series is called the virial expansion. It reads:

$$P = nk_B T (1 + B_2 n + B_3 n^2 + \dots) \quad (4.5)$$

where B_n is the n^{th} **virial coefficients**. Injecting Eq. (4.4) into the partition function, we obtain

$$Z = \frac{1}{N! \Lambda^{3N}} \int \prod_{i=1}^N d^3 \vec{q}_i \underbrace{\left[1 + \sum_{i < j} f_{ij} + \sum_{i < j} \sum_{n < p} f_{ij} f_{kl} + \dots \right]}_{2^{N(N-1)/2} \text{ terms}} \quad (4.6)$$

where the $2^{N(N-1)/2}$ terms comes from expanding the product $\prod_{i < j} (1 + f_{ij})$.

While Eq. (4.6) seems terrifying, progress can be made by grouping similar terms into a **cluster expansion**. The idea is to turn Eq. (4.6) into a sum of integrals with varying numbers of factors f_{ij} and to represent the various terms in the sum as different graphs (or diagrams) with a number of nodes equal to the number of particles N . When a factor f_{ij} is present in an integral, we connect particles i and j on the graph. Each diagram can be decomposed into connected clusters, which allows for a useful factorization of the overall. We can then define coefficients b_n that contains all the contributions from connected clusters with n particles. For instance:

$$b_1 = \int d\vec{q}_1 = V \quad (4.7)$$

$$b_2 = \int d\vec{q}_1 d\vec{q}_2 f(\vec{q}_1 - \vec{q}_2) = V \int dq f(q); \quad (4.8)$$

$$b_3 = \int d\vec{q}_1 d\vec{q}_2 d\vec{q}_3 f(\vec{q}_1 - \vec{q}_2) f(\vec{q}_2 - \vec{q}_3) f(\vec{q}_3 - \vec{q}_1) + \int d\vec{q}_1 d\vec{q}_2 d\vec{q}_3 f(\vec{q}_1 - \vec{q}_2) f(\vec{q}_2 - \vec{q}_3) \quad (4.9)$$

$$+ \int d\vec{q}_1 d\vec{q}_2 d\vec{q}_3 f(\vec{q}_1 - \vec{q}_2) f(\vec{q}_3 - \vec{q}_1) + \int d\vec{q}_1 d\vec{q}_2 d\vec{q}_3 f(\vec{q}_2 - \vec{q}_3) f(\vec{q}_3 - \vec{q}_1) \\ = V \left[\int d\vec{q} d\vec{k} f(\vec{q}) f(\vec{k}) f(-\vec{q} - \vec{k}) + 3 \int d\vec{q} f(\vec{q}) \int d\vec{k} f(\vec{k}) \right]; \quad (4.10)$$

We refer to Sec. 5-2 of [2] for the full derivation and report directly the result:

$$Z = \frac{1}{N! \Lambda^{3N}} \sum_{n_\ell \text{ s.t. } N = \sum_\ell n_\ell \ell} \prod_\ell b_\ell^{n_\ell} \times \underbrace{\frac{N!}{\prod_k (k!)^{n_k} n_k!}}_{\text{combinatorial}} \quad (4.11)$$

where the sum is on the number of cluster n_ℓ with ℓ connected nodes, constrained to the fact that the total number of nodes equals the particle number (in the canonical ensemble). The final factor is a combinatorial term which takes into account the **indistinguishable** nature of the particles. Since it is

difficult to deal with a constrained sum, we conveniently switch to the grand canonical ensemble, where the number of particles is allowed to vary. The **grand canonical partition function** reads:

$$Q = \sum_N e^{\beta\mu N} Z_N = \sum_{\{n_\ell\}} \prod_{\ell=1}^{\infty} b_\ell^{n_\ell} \left(\frac{e^{\beta\mu}}{\Lambda^3} \right)^{\sum_\ell n_\ell \ell} \times \prod_{\ell=1}^{\infty} \frac{1}{(\ell!)^{n_\ell} n_\ell!} \quad (4.12)$$

$$= \prod_{\ell=1}^{\infty} \sum_{n_\ell=0}^{\infty} \left(b_\ell \frac{z^\ell}{\ell!} \right)^{n_\ell} \frac{1}{n_\ell!} \quad (4.13)$$

$$= \prod_{\ell=1}^{\infty} \exp \left[\frac{b_\ell}{\ell!} z^\ell \right], \quad (4.14)$$

where we have introduced the rescaled fugacity

$$z = \frac{e^{\beta\mu}}{\Lambda^3}. \quad (4.15)$$

From there, the **grand potential** reads:

$$G = -k_B T \ln Q = -k_B T \sum_{\ell=1}^{\infty} z^\ell \frac{b_\ell}{\ell!} = -PV. \quad (4.16)$$

where the final equality applies in the large size limit and assume that G is extensive. We can then express the pressure as a series in the chemical potential μ :

$$P(\mu) = k_B T \sum_{\ell=1}^{\infty} \left(\frac{e^{\beta\mu}}{\Lambda^3} \right)^\ell \frac{\bar{b}_\ell}{\ell!} \quad (4.17)$$

where $\bar{b}_\ell = \frac{b_\ell}{V}$ is intensive since $b_\ell \propto V$, as can be checked in Eqs. (4.7)-(4.10).

Equation (4.17) thus gives us P in terms of the chemical potential μ or the fugacity z . To get P as a series in n , we thus need to express n as a function of z , and to invert this relation to get $z(n)$, that we will finally inject in Eq. (4.17). This is a standard method to compute the equation of state perturbatively, that we will also use in quantum statistical mechanics.

First, we recall that $\langle N \rangle = -\frac{\partial G}{\partial \mu}$. Combining this with Eq. (4.16), one gets $n = \frac{N}{V}$ as a power series in z :

$$n = \sum_{\ell=1}^{\infty} \left(\frac{e^{\beta\mu}}{\Lambda^3} \right)^\ell \frac{\bar{b}_\ell}{(\ell-1)!} = z + \bar{b}_2 z^2 + \frac{\bar{b}_3}{2} z^3 + \dots \quad (4.18)$$

We can invert the series in Eq. (4.18) by introducing the *ansatz* $z(n) = \sum_{k=0}^{\infty} c_k n^k$ and solving order by order in n . One finds:

$$z = n - \bar{b}_2 n^2 + \left(2\bar{b}_2 - \frac{\bar{b}_3}{2} \right) n^3 + \mathcal{O}(n^4) \quad (4.19)$$

which gives the **virial expansion** for the pressure:

$$\beta P = n - \frac{\bar{b}_2}{2} n^2 + \left[\bar{b}_2^2 - \frac{\bar{b}_3}{3} \right] n^3 + \mathcal{O}(n^4) \quad (4.20)$$

Using Eq. (4.8), we find the second virial coefficient:

$$B_2 = -\frac{1}{2} \int d\vec{q} \left(e^{-\beta v(\vec{q})} - 1 \right) \quad (4.21)$$

Approximate expression of B_2 for the Lennard-Jones potential. To get a simpler expression of B_2 , we approximate the interaction potential as:

$$v(r) = \begin{cases} \infty, & \text{if } r < d. \\ -v_0 \left(\frac{d}{r}\right)^6, & \text{if } r > d. \end{cases} \quad (4.22)$$

which gives:

$$B_2 = -\frac{1}{2} \left[-\frac{4}{3}\pi d^3 + \int_d^\infty 4\pi r^2 dr \left(e^{\beta v_0 (d/r)^6} - 1 \right) \right] \quad (4.23)$$

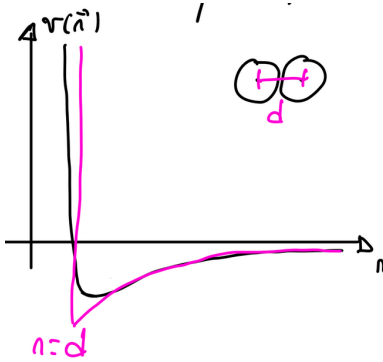


Figure 4.3: Sketch of the approximated interaction potential.

At **high temperature**, $\beta v_0 \ll 1$ and we can expand the integrand:

$$\int_d^\infty 4\pi r^2 dr \left(e^{\beta v_0 (d/r)^6} - 1 \right) \simeq 4\pi \beta v_0 d^6 \left[\frac{-r^{-3}}{3} \right]_d^\infty = \frac{4\pi d^3}{3} \frac{v_0}{k_B T}. \quad (4.24)$$

The second virial coefficient can thus be approximated as:

$$B_2 = \frac{\Omega}{2} \left[1 - \frac{v_0}{k_B T} \right] \quad (4.25)$$

with $\Omega = \frac{4\pi d^3}{3}$ the **volume excluded** due to the **short range repulsive interactions**, as illustrated on Fig. 4.4.

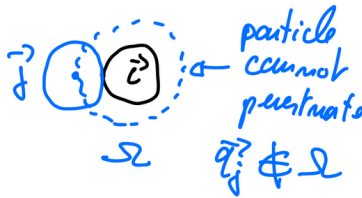


Figure 4.4: Ω is the volume around a particle which is not accessible to other particles due to the excluded volume interactions.

All in all, the **virial expansion** for the pressure thus reads:

$$P = nk_B T \left[1 + \underbrace{\frac{n\Omega}{2} \left(1 - \frac{v_0}{k_B T} \right)}_{\text{first correction to ideal gas}} \right]. \quad (4.26)$$

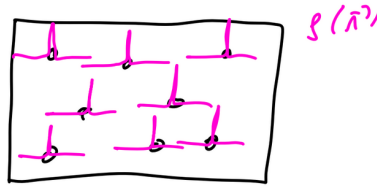


Figure 4.5: The microscopic density field is a combination of Dirac distributions, each centered on the position of a different particle.

Let us make some comments on our results so far.

- The expansion in n is actually an expansion in $n\Omega$, which is the average number of particles that would be in the volume Ω in the absence of exclusion forces.
- Ω^{-1} is the density at which particles are essentially touching, which is a good approximation of the liquid density at low temperatures, so that $n\Omega \simeq \frac{n}{n_L}$. This means that the virial expansion converges rapidly if $n \ll n_L$. For $n \simeq n_L$ we need other methods/expansions (see [1]).
- To expand $e^{-\beta v_0} \simeq 1 - \beta v_0$ we need $\beta v_0 \ll 1$, which is only true at high temperature. To check the thermodynamic stability of the expansion at low temperatures, we take the derivative of the pressure with respect to V of Eq. (4.26) and find:

$$\frac{\partial P}{\partial V} > 0 \quad \text{if} \quad k_B T < v_0 \frac{N\Omega}{V + N\Omega} \quad (4.27)$$

The expansion thus suggests a negative compressibility of the fluid, $\kappa = -\frac{1}{V} \frac{\partial V}{\partial P} < 0$, at low temperatures, which corresponds to a **thermodynamic instability** of the system. Indeed, a negative compressibility means that a spontaneous fluctuation of the volume of the system $V \rightarrow V - \delta V$ induces a reduction of the internal pressure $P \rightarrow P - \delta P$, which itself leads to a further compression of the system and to an eventual collapse.

To understand what happens at low temperatures, let us now develop an alternative approach to our problem of interacting particles.

4.1.2 Mean-field theory and van der Waals equation

First, we introduce the **empirical density field** (see Figure 4.5):

$$\rho(\vec{r}) = \sum_{i=1}^N \delta(\vec{q}_i - \vec{r}) \quad (4.28)$$

which allows us to express the potential energy as:

$$U = \frac{1}{2} \sum_{i \neq j} v(\vec{q}_i - \vec{q}_j) = \frac{1}{2} \int d\vec{q} d\vec{k} v(\vec{q} - \vec{k}) \rho(\vec{q}) \rho(\vec{k}) \quad (4.29)$$

where we have set $v(0) = 0$.

Mean-field approximation: Let us now *assume* that the system is homogeneous and that particles are uncorrelated. We thus approximate the density as uniform, $\rho(\vec{r}) \simeq \rho_0$, while enforcing the excluded volume interactions:

$$U = \frac{1}{2} \int d\vec{q} \left[\rho(\vec{q}) \underbrace{\int_{|\vec{q}-\vec{k}|>d} d\vec{k} v(\vec{q}-\vec{k}) \rho(\vec{k})}_{-\rho_0 u} \right] = -\frac{\rho_0 u}{2} \int d\vec{q} \rho(\vec{q}) \quad (4.30)$$

$$= -\frac{V}{2} \rho_0^2 u = -\frac{N^2 u}{2V} \quad (4.31)$$

where we have introduced $u = \int_{|\vec{r}|>d} v(\vec{r}) d\vec{r}$, which measures the strength of the attractive tail of the interaction potential.

In the mean-field approximation, the canonical partition function becomes:

$$Z = \frac{1}{N! \Lambda^{3N}} \int_{\text{excl. vol.}} d\vec{q}_1, \dots, d\vec{q}_N e^{\beta \frac{N^2 u}{2V}}, \quad (4.32)$$

where the integral limits must respect the excluded volume between particles. If we neglect correlation between particles, the first particle has access to a volume V , the second particle to $V - \Omega$, the third to $V - 2\Omega$ provided the two first particles are not close to each other, etc. leading to

$$\int_{\text{excl. vol.}} d\vec{q}_1, \dots, d\vec{q}_N = V(V - \Omega) \dots (V - (N - 1)\Omega). \quad (4.33)$$

To leading order in Ω/V , this leads to

$$Z = \frac{V^N e^{\beta \frac{N^2 u}{2V}}}{N! \Lambda^{3N}} \underbrace{\left[1 - \frac{\Omega}{V} (1 + 2 + \dots + N - 1) + \mathcal{O}\left(\frac{\Omega^2}{V^2}\right) \right]}_{\simeq (1 - \frac{n}{2} \Omega N) \simeq (1 - \frac{n\Omega}{2})^N} \quad (4.34)$$

$$= \underbrace{\frac{1}{N! \Lambda^{3N}}}_{\text{kinetic energy}} \times \underbrace{e^{\beta \frac{N^2 u}{2V}}}_{\text{attraction}} \times \underbrace{\left(V - \frac{N\Omega}{2} \right)^N}_{\text{exclusion}} \quad (4.35)$$

One of the nice features of this expression for Z is that the respective contributions of the kinetic energy, attractive interactions, and excluded volume are all singled out.

For a homogeneous system, the pressure is thus given by:

$$P_H = k_B T \frac{\partial \ln Z}{\partial V} = \frac{N k_B T}{V - \frac{N\Omega}{2}} - \beta \frac{N^2 u}{2V^2} \quad (4.36)$$

which corresponds to the celebrated **van der Waals equation**. One can easily check that the cluster expansion is consistent with the mean-field approach and the van der Waals equation up to the second virial coefficient. While this agreement validates the mean-field approach, it also tells us that both approaches suffers from a problematic behavior at low temperatures.

Indeed, at low temperature the system undergoes a phase separation and the hypothesis of homogeneity breaks down. To make progress, it is convenient to introduce the **free volume per particle** $\tilde{v} = \frac{V}{N}$ and express the pressure as:

$$P = \frac{k_B T}{\tilde{v} - \frac{\Omega}{2}} - \frac{u_0 \Omega}{2\tilde{v}^2}. \quad (4.37)$$

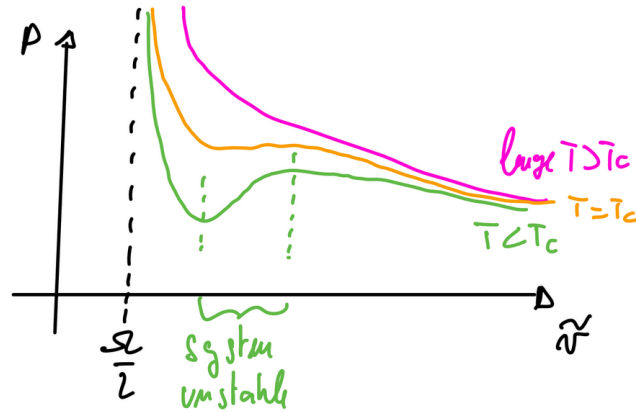


Figure 4.6: Example of three isotherms for $T > T_c$, $T = T_c$, and $T < T_c$. At the critical temperature the pressure displays an inflection point at some critical free volume \tilde{v}_c . At low temperatures, $T < T_c$ there is an unstable region where the compressibility is negative. This region is not accessible to the system, and the system phase separates instead.

One sees that the first term is the leading contribution at large temperature T and at large \tilde{v} , while the second term becomes important at small T and \tilde{v} . Below a critical temperature T_c the competition between these two terms leads to a non-monotonous behavior of the pressure shown in Figure 4.6.

In the region where $P'(\tilde{v}) > 0$, the compressibility is negative and the system becomes unstable. Looking back at our computation, we see that an important assumption we made is that the system is homogeneous. Note that if, instead, the system undergoes phase separation between a gas phase where \tilde{v} is locally large and a liquid phase where \tilde{v} is locally small, then both parts of the system will be in regions of the isotherm where the compressibility is positive.

How to describe phase separated states? Consider a **macrostate** defined by the density field $\rho(\vec{r})$ and build the probability $P(\rho(\vec{r}))$ in the canonical ensemble. Compare the probability of a profile $\rho_{ps}(\vec{r})$ separated between a gas region and a liquid region and the probability of the homogeneous solution ρ_0 . If $P(\rho_{ps}) \gg P[\rho_0]$, then the system phase separates (see Pset 7, exercise 1).

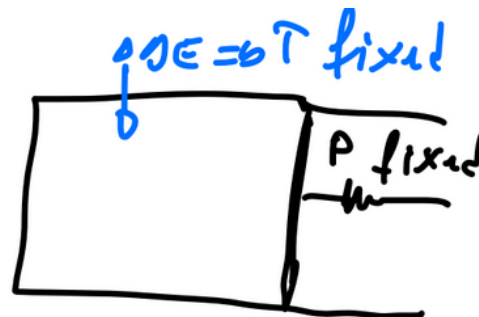


Figure 4.7: In the isobaric Gibbs ensemble, the independent variables are N , T and P .

An alternative approach: the isobaric Gibbs ensemble. As an exercise, you can start from the canonical ensemble and derive the probability distribution in the isobaric ensemble by switching from the volume

V , as a control parameter, to the pressure P (See Fig. 4.7). The result is:

$$P(\mathcal{C}) = \frac{1}{Z_I} e^{-\beta E(\mathcal{C}) - \beta PV} \quad (4.38)$$

with the isobaric partition function:

$$Z_I(P, T, N) = \int_0^\infty dV e^{-\beta PV} Z_c(V, T, N) = \int_0^\infty dV e^{-\beta[PV + F]} = \int_0^\infty dV e^{-\beta N[P\tilde{v} + f(\tilde{v}, T) + \mathcal{O}(1/N)]} \quad (4.39)$$

where $f(\tilde{v}, T) = \lim_{N \rightarrow \infty} \frac{F}{N}$ is the large N limit of the free energy density. As we have done many times, we can use the saddle point approximation to express Z_I in the large N limit as:

$$Z_I \sim e^{-\beta N[P\tilde{v}^* + f(\tilde{v}^*, T)]} = e^{-\beta[PV^* + F(V^*, T)]} \quad (4.40)$$

where $V^* = N\tilde{v}^*$ and

$$\tilde{v}^* = \underset{\tilde{v}}{\operatorname{argmin}}[\hat{\mu}(\tilde{v})] \quad \text{with} \quad \hat{\mu}(\tilde{v}) \equiv PV + f(\tilde{v}, T). \quad (4.41)$$

As usual with large-size limits, the probability distribution of the free volume satisfies $P(\tilde{v}) \underset{N \rightarrow \infty}{\sim} \delta(\tilde{v} - \tilde{v}^*)$ where \tilde{v}^* minimizes $\hat{\mu}(\tilde{v})$ so that \tilde{v} solves:

$$P = -\frac{\partial f}{\partial \tilde{v}} = -\frac{\partial F}{\partial V}. \quad (4.42)$$

In the canonical ensemble, we saw that $\hat{F}(E) = E - TS(E)$ is sometimes called a non-equilibrium free energy because, in the large size limit, $F(\beta) = \hat{F}(E^*)$, with $E^* = \underset{E}{\operatorname{argmin}}[\hat{F}(E)]$. Similarly, $\hat{\mu}$ is sometimes called a non-equilibrium chemical potential. Indeed, for large systems, $PV + F = F - G = F - (F - \mu N) = \mu N$. In the large size limit, we thus have $\mu = \hat{\mu}(\tilde{v}^*)$. We stress that $\hat{\mu}$ truly becomes the chemical potential only in the large system size, when $V \rightarrow V^*$.

In the isobaric ensemble, P is fixed externally. To solve for \tilde{v}^* and determine the state of the system, we thus need an expression for $-\frac{\partial F}{\partial V}$ in terms of \tilde{v} to solve Eq. (4.42). A natural route is to assume that the system is homogeneous so that we can use the mean-field approximation:

$$-\frac{\partial F}{\partial V} = P_H(\tilde{v}) \quad (4.43)$$

with P_H given by Eq. (4.37). In Fig. 4.8, we can plot $P_H(\tilde{v})$ for different temperatures T .

We now focus on the case where $T < T_c$ so that the function P_H is non-monotonous and there are three distinct solutions to Eq. (4.43). In Fig. 4.9, we plot $\hat{\mu}(\tilde{v})$ for different values of the pressure at this temperature. At large (P_3) and small (P_1) pressures, there is a unique solution to Eq. (4.43) and the system is in a homogeneous phase at the corresponding free volume \tilde{v}_i . In the intermediate pressure regime, we see that the multiple solutions to Eq. (4.43) correspond to local extrema of $\hat{\mu}(\tilde{v})$. The value of \tilde{v} that dominates the integral in Eq. (4.40) is then the global minimum of the chemical potential. For most values of P , there will be a unique minimum and the system is in the corresponding homogeneous state. At a given value $P_t(T)$, the two minima of $\hat{\mu}$ have the same value (see Figure 4.10): the system cannot decide which phase is the most favorable and one observes a discontinuous transition. For $P = P_t(T) - \varepsilon$, the system is in the dilute gas phase while for $P = P_t(T) + \varepsilon$, the system is in the dense liquid phase, for any finite value $\varepsilon > 0$. The free volume \tilde{v} (or the density $n = \tilde{v}^{-1}$) thus jumps discontinuously at $P_t(T)$.

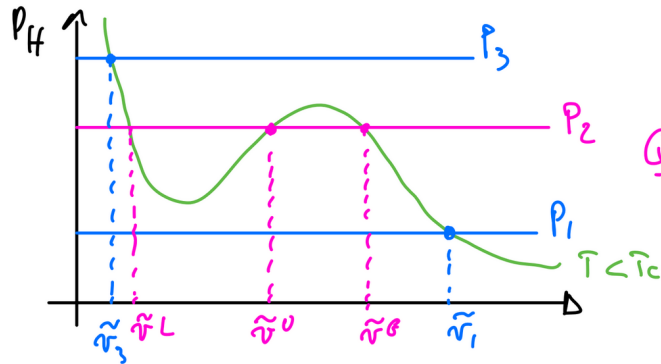


Figure 4.8: Example of isotherm curve $P_H(\tilde{v})$ at a low temperature $T < T_c$. The intersects with the value of pressure P_2 fixed by the isobaric ensemble identify three solutions to Eq. (4.43).

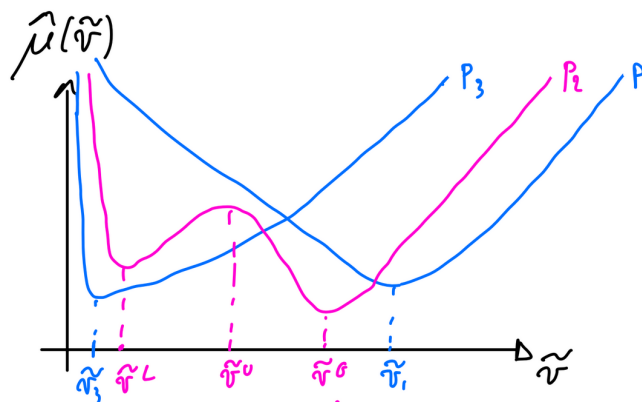


Figure 4.9: The pressure P_2 identified in the previous figure, corresponds to a non-convex function $\hat{\mu}(\tilde{v})$. In the thermodynamic limit, the system favors the global minimum of \tilde{v} .

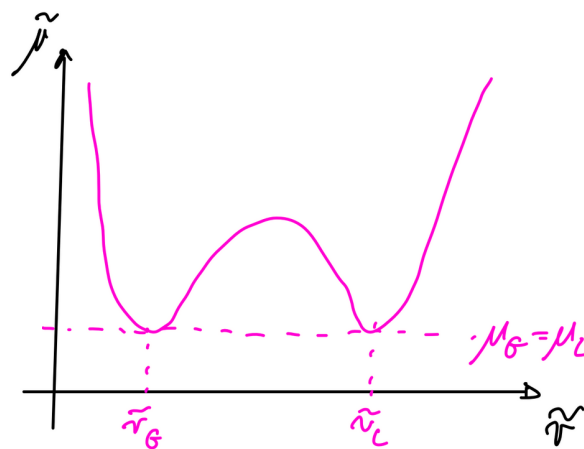


Figure 4.10: At the transition pressure $P_t(T)$, the chemical potential has two degenerate minima. The system cannot choose between gas and liquid phases and one observes one or the other depending on the preparation. There are also strong hysteresis loops if one ramps the pressure up and down around $P_t(T)$.

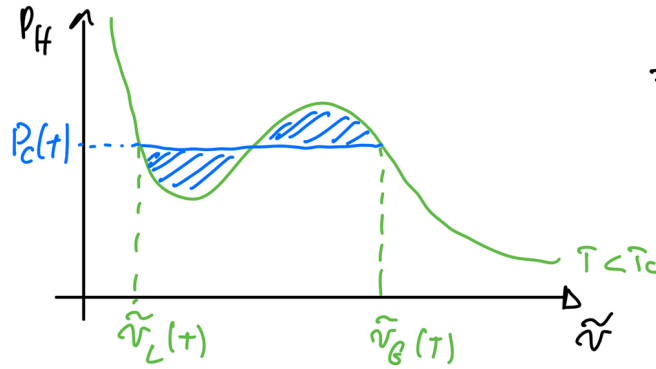


Figure 4.11: Graphically the critical pressure $P_c(T)$ can be obtained by finding the line which gives equal areas on both sides of the inflection point.

Since the first derivative of G with respect to volume is discontinuous, we say that the system undergoes a first order phase transition.

How do we determine $P_t(T)$? To determine the value $P_t(T)$, we require that the two minima of $\hat{\mu}$ are equal: $\hat{\mu}(\tilde{v}_G) = \hat{\mu}(\tilde{v}_L)$. Using the definition (4.41), we find

$$\hat{\mu}(\tilde{v}_G) - \hat{\mu}(\tilde{v}_L) = \int_{\tilde{v}_L}^{\tilde{v}_G} d\tilde{v} \frac{d\hat{\mu}}{d\tilde{v}} \quad (4.44)$$

$$= \int_{\tilde{v}_L}^{\tilde{v}_G} d\tilde{v} (P_t - P_H(\tilde{v})) = 0 \quad (4.45)$$

The value of P_t is thus such that the area between P_t and P_H integrates to zero on the interval $[\tilde{v}_L, \tilde{v}_G]$. This is the celebrated **Maxwell construction** shown in Figure 4.11.

Canonical ensemble. In the canonical ensemble, since N and N are both constant, the system cannot jump from the liquid to the gas phase. Instead, it phase separates between the gas and liquid binodals. These densities are selected such that gas and liquid phases have equal pressure and equal chemical potential. The real pressure is thus constant in the phase separated state (see Figures 4.12 and (4.13)).

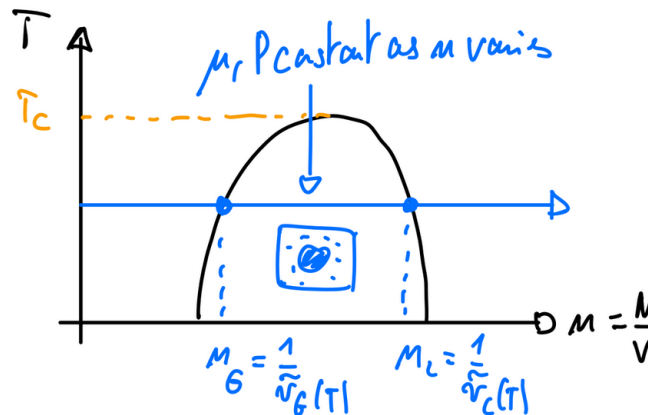


Figure 4.12: In the phase-separated region of the phase diagram, the pressure P and the chemical potential μ are constant along isotherms, as the local density varies. They are equal to $P_t(T)$ and $\hat{\mu}(\tilde{v}_G) = \hat{\mu}(\tilde{v}_L)$.

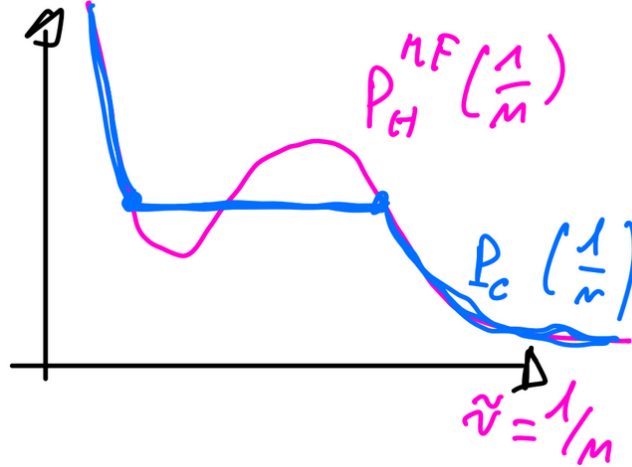


Figure 4.13: In the canonical ensemble, we can vary the free volume \tilde{v} by changing the density $1/n$ and measure the corresponding pressure. In the homogeneous phase, one observes $P(n) = P_H(n)$ (up to corrections due to the fluctuations neglected in the mean-field approximation). In the phase-separated region, $P(n) = P_t(T)$ is constant. The region of negative compressibility is thus never seen by the system.

Universality: Let us examine the behavior of the system near the critical point. At temperature T_c and volume V_c the isotherm $P_H(\tilde{v})$ has an inflection point, implying

$$\frac{\partial P}{\partial \tilde{v}} = \frac{\partial^2 P}{\partial \tilde{v}^2} = 0 \quad \text{at } T_c, V_c \quad (4.46)$$

By imposing these conditions on the mean-field expression Eq. (4.37), we obtain:

$$\frac{\tilde{v}_c^3}{u_0} = \frac{(\tilde{v}_c - \Omega/2)^2}{k_B T_c} \quad (4.47)$$

$$\frac{\tilde{v}_c^4}{3u_0} = \frac{(\tilde{v}_c - \Omega/2)^3}{2k_B T_c} \quad (4.48)$$

Taking the ratio of these two equations yields $\tilde{v}_c = \frac{3\Omega}{2}$. Substituting this result, we find $k_B T_c = \frac{8u_0}{27\Omega}$. This analysis reveals a one-to-one correspondence between the model parameters, Ω and u_0 , and the critical parameters T_c and \tilde{v}_c . Importantly, this relationship leads to a **parameter-free relation** which can be tested in simulations and experiments:

$$\frac{P_c \tilde{v}_c}{k_B T_c} = \frac{3}{8}. \quad (4.49)$$

In experimental studies of simple atomic fluids, many systems yield values of $\frac{P_c \tilde{v}_c}{k_B T_c}$ in the range $[0.28, 0.33]$. This suggests that, while this ratio is not strictly universal, it is remarkably consistent across different systems. Another prediction from the mean-field theory, obtained by taking a Taylor expansion of Eq. (4.37) is,

$$P - P_c \propto (\tilde{v} - \tilde{v}_c)^3 \quad (4.50)$$

In experiments, one finds $P - P_c \propto (\tilde{v} - \tilde{v}_c)^\delta$, with $\delta \simeq 5$ for all simple gases. This time, the value of the exponent is wrong, but the exponent itself is a universal quantity!

We can also compute the **compressibility**, $\kappa = -\frac{1}{\bar{v}} \frac{\partial \bar{v}}{\partial p}$. Near the critical temperature, our mean-field theory predicts: $\kappa \propto (T - T_c)^{-1}$. Again, experiments find a universal exponent $\kappa \propto (T - T_c)^{-\gamma}$, with $\gamma \simeq 1.24$, which is close to, but distinct from the mean-field exponent.

We thus observe two surprises:

- There are **universal properties**, that are identical among quite different systems and models. This is why the "simple models" studied in statistical mechanics are so useful: there are many properties that are common to a simulation with a Lennard Jones potential and an experiment!
- Mean-field theory does not predict those properties quantitatively, because **fluctuations** are important and have been neglected. The approximation $\rho(\vec{r}) \simeq \rho_0$ is too simple.

Understanding the physical origin of universality and correcting the mean-field exponents is something you will learn in the 8.334 class!

4.2 The ferromagnetic transition & the mean-field Ising model

The Ising model is a simplified model to account for the emergence of ferromagnetism as a result of the exchange interactions between electrons in a solid. Consider a lattice of L^d sites in d dimensions. To each site, we associate a value $S_i \in \{+1, -1\}$ (which corresponds to the $\pm 1/2$ electronic spins) and consider the Hamiltonian:

$$H = -J \sum_{i \vee j} S_i S_j - \hat{h} \mu \sum_i S_i \quad (4.51)$$

where J is the coupling constant (the exchange energy), \hat{h} is a magnetic field, μ is the magnetic moment of the electrons (for simplicity we denote $h \equiv \mu \hat{h}$) and $\sum_{i \vee j}$ runs over all pairs of nearest neighbors. A configuration of the system is described by the values of $\{S_i\}$, so that there are 2^N possible configurations, where $N = L^d$ is the number of spins. When $J = 0$, the spins are non-interacting and the system can be treated as a collection of non-interacting two-level systems. The Hamiltonian in Eq. (4.51) shows that the spins tend to align with h . This is called **paramagnetism** and the system's magnetization $M = \sum_{i=1}^N S_i$ tends to align with h .

Here we want to understand **ferromagnets**, a name that encompasses systems that develop a spontaneous magnetization at low temperature in the absence of magnetic field. In such systems, there exists a temperature T_c , called the Curie temperature, such that,

$$\text{for } T < T_c, \quad \lim_{N \rightarrow \infty} \langle |m| \rangle = \lim_{N \rightarrow \infty} \left\langle \frac{1}{N} \left| \sum_{i=1}^N S_i \right| \right\rangle > 0. \quad (4.52)$$

For such systems, the exchange interaction between electrons thus leads to an **emergent** magnetization. Ferromagnets corresponds to systems with $J > 0$, which favors energetically the alignment of nearest neighbors, $\uparrow\uparrow$ & $\downarrow\downarrow$, whereas $J < 0$ corresponds to antiferromagnets, which favors antialigned configurations, $\uparrow\downarrow$ & $\downarrow\uparrow$. These systems are also very interesting, but we will not study them here.

Canonical ensemble: At $T = \infty$, the Hamiltonian is irrelevant and the Boltzmann weight is identical for all configurations, $P(\{S_i\}) = \frac{1}{2} = 2^{-N}$. Since all configurations are equally likely, M is the sum of N

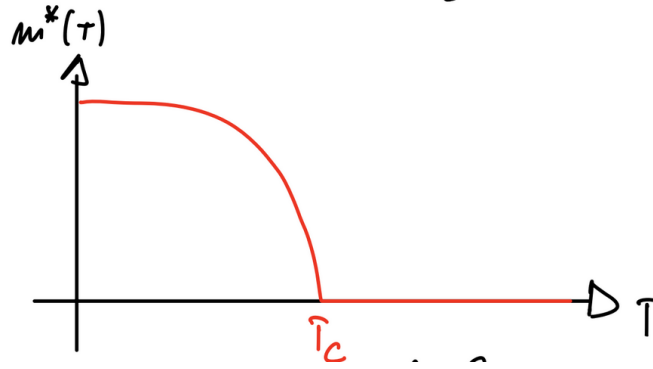


Figure 4.14: Schematic representation of the norm of the magnetization as a function of the temperature, showing the existence of a phase transition at the Curie temperature T_c .

uncorrelated random variables and scales as \sqrt{N} , so that $m^* = \langle |m| \rangle \sim 1/\sqrt{N}$ vanishes as $N \rightarrow \infty$. On the other hand, at $T = 0$, $P(\{S_i\}) = 0$ if all spins are not aligned, and the magnetization m is either $+1$ or -1 . The question we want to address is what happens between these two extreme cases?

Let's keep h finite for now, and write the partition function:

$$Z = \sum_{\{S_i\}} e^{\beta [J \sum_{i \vee j} S_i S_j + h \sum_i S_i]} \quad (4.53)$$

so that $\langle M \rangle = \frac{\partial}{\partial(\beta h)} \ln Z|_{h=0}$ (keeping βJ constant), which leads to

$$\langle m \rangle|_{h=0} = \frac{k_B T}{N} \frac{\partial}{\partial h} \ln Z \Big|_{h=0}. \quad (4.54)$$

The computation of Z can be worked out analytically in $1D$ using the method of transfer matrix and in $2D$ (at $h = 0$). The $2D$ computation is due to an analytical tour de force by Onsager in 1942. (Simpler derivations were later proposed, for instance making use of the Wigner-Jordan transformation.) In $3D$ there is no analytical solution but extensive numerics give us a very good understanding of the physics.

The result is illustrated in Figure 4.14 which shows that $m^*(T)$ has a singular behaviour at $T = T_c$. Above the Curie temperature, the averaged magnetization is identically zero. Below the critical temperature T_c , $m = \pm m^*(T) \sim \mathcal{O}(1)$. As $L \rightarrow \infty$, the probability density of m approaches a distribution given by the superposition of two Dirac's distributions, $P(m) \rightarrow \frac{1}{2}\delta(m + m^*) + \frac{1}{2}\delta(m - m^*)$. Let us now try to account for this phenomenology.

Mean-field theory: Let us consider the contribution of spin i to the Hamiltonian, namely $H_i = -h S_i - (J \sum_{i \vee j} S_j) S_i$. The term $J \sum_{i \vee j} S_j$ can thus be seen as the effective magnetic field that the neighbors of i induce on spin i . If the system is homogeneous and the fluctuations are small, we can approximate

$$\sum_{i \vee j} S_j \simeq qm \quad (4.55)$$

where q is the number of neighbors of spin i ($= 2D$ on a square lattice in D dimensions) and m is the average magnetization. This leads to

$$H_i = -(h + qmJ) S_i \quad (4.56)$$

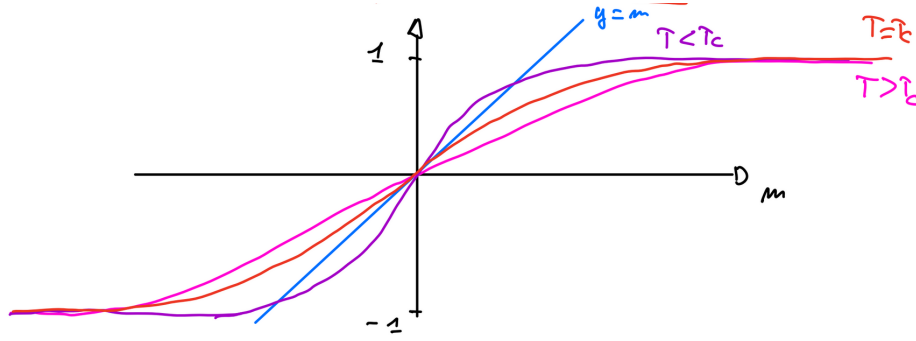


Figure 4.15: Caption

which is the Hamiltonian of a single spin in an effective magnetic field $h_{\text{eff}} = h + qmJ$. We can then compute the resulting average magnetization of spin i :

$$\bar{m}(h_{\text{eff}}) \equiv \langle m \rangle_{h=h_{\text{eff}}} , \quad (4.57)$$

and then make sure that the mean-field approximation is self-consistent, i.e. that

$$\bar{m}(h_{\text{eff}}(m)) = m . \quad (4.58)$$

Equation (4.58) can be understood as follows: because of the average magnetization m of my neighbors, I get an average magnetization \bar{m} . But since I am the neighbor of my neighbor, I contribute to exerting on them a magnetic field and they need to have an average magnetization consistent with mine, so that we need $m = \bar{m}$.

Using the **partition function** $Z_{\text{eff}}^1 = e^{-\beta(h+qmJ)} + e^{\beta(h+qmJ)}$, we compute:

$$\bar{m}(\beta_{\text{eff}}) = \frac{\partial}{\partial(\beta h)} \ln \left[e^{\beta(h+qmJ)} + e^{-\beta(h+qmJ)} \right] \quad (4.59)$$

$$= \tanh [\beta (h + qmJ)] \quad (4.60)$$

We then set $h = 0$ and solve the self-consistency equation:

$$m = \tanh [\beta qmJ] . \quad (4.61)$$

Plotting the function $y = m$ and $y = \tanh(\beta Jqm)$ in Fig. 4.15 helps understanding the physics of the system. For $T > T_c$, the only solution is $m = 0$, because the slope of $\tanh(\beta Jqm)$ is smaller than 1 at zero and the functions never cross again. For $T < T_c$, the slope of $\tanh(\beta Jqm)$ is larger than 1 at $m = 0$ and the functions have to cross again. There are thus three solutions: $m = \pm m^*$ and $m = 0$. As for the intermediate solution \tilde{v} for the liquid-gas transition, the intermediate solution $m = 0$ is never observed. To show this, one can construct the probability density $P(m)$ and show that $m = 0$ is a local minimum of $P(m)$ for $T < T_c$.

Near the critical temperature T_c we can expand $\tanh(x) \underset{x \rightarrow 0}{\simeq} x$, to get

$$m = \beta qmJ \quad (4.62)$$

At the transition point, the slope of $\tanh(q\beta Jm)$ goes from being less than 1 to being more than 1, so that at T_c it has slope 1 and:

$$\beta_c = \frac{1}{qJ} \quad \Leftrightarrow \quad T_c = \frac{qJ}{k_B}. \quad (4.63)$$

Critical exponent: Expanding $\tanh(x) \simeq x - \frac{x^3}{3}$, we see that

$$m \simeq \beta qmJ - \frac{(\beta qmJ)^3}{3} \quad (4.64)$$

$$\Leftrightarrow (\beta - \beta_c)qJ = \frac{1}{3}\beta^3 q^3 J^3 m^3 \quad (4.65)$$

$$\Leftrightarrow m \propto (\beta - \beta_c)^{1/2} \quad (4.66)$$

Since $m = 0$ for $T > T_c$, we see that m is continuous at T_c but $m'(T)$ is singular. We say that the system undergoes a second order phase transition since the second order derivative of $\ln Z$ is discontinuous.

The mean-field theory correctly predicts the existence of a singularity in the curve $m(T)$ at the critical temperature but, as for the liquid-gas coexistence, it gets the exponent wrong. For instance, in $2D$, one finds $m \sim |T - T_c|^\alpha$ with $\alpha = 1/8$).

Restoring a finite magnetic field $h \neq 0$, expanding the self-consistency relation leads to

$$m \simeq \beta h + m \frac{T_c}{T} - \frac{m^3}{3} \left(\frac{T_c}{T} \right)^3 \quad (4.67)$$

At $T = T_c$, $m \propto h^{1/3}$ while for $T \neq T_c$, the **susceptibility** scales as

$$\chi = \left. \frac{\partial m}{\partial h} \right|_{h=0} \sim \frac{1}{T - T_c} \quad (4.68)$$

This is the same exponent as that predicted for the compressibility of the interacting fluid in the mean-field theory of the liquid-gas phase transition. There is a deep reason behind that: defining $n_i = \frac{1+S_i}{2} \in [0, 1]$, one maps the Ising model on a *lattice-gas model* of attractive particles. The Ising model and the liquid-gas transition are thus in the same universality class! As you will discover if you follow 8.334, the world of phase transitions and critical phenomena is full of such surprises.

Bibliography

- [1] Jean-Pierre Hansen and Ian Randal McDonald. *Theory of simple liquids: with applications to soft matter*. Academic press, 2013.
- [2] Mehran Kardar. *Statistical physics of particles*. Cambridge University Press, 2007.